

Phenothiazine Decorated Carbazoles: Effect of Substitution Pattern on the Optical and Electroluminescent Characteristics

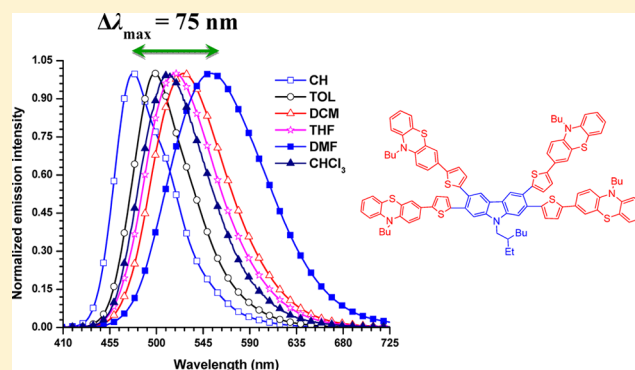
Rajendra Kumar Konidena,[†] K. R. Justin Thomas,^{*,†} Sudhir Kumar,[‡] Ya-Chi Wang,[‡] Chieh-Ju Li,[‡] and Jwo-Huei Jou[‡]

[†]Organic Materials Laboratory, Department of Chemistry, Indian Institute of Technology Roorkee, Roorkee-247 667, India

[‡]Department of Material Science and Engineering, National Tsing Hua University, Hsinchu 30013, Taiwan

Supporting Information

ABSTRACT: A series of thienylphenothiazine decorated carbazoles were synthesized and characterized by optical, electrochemical, thermal, and theoretical investigations. Absorption spectra of the compounds are influenced by the substitution pattern and chromophore number density. Compounds containing 2,7-substitution exhibited red-shifted absorption, while the chromophore loading on the other positions led to the increment in molar extinction coefficients due to the increase in the chromophore density. Multiple substitutions resulted in twisting of chromophores and affected the conjugative delocalization of the π -electrons, which produced shorter wavelength absorption for the 2,3,6,7-tetrasubstituted derivative. Interestingly, the compounds exhibited excited-state solvatochromism attributable to the structural reorganization-induced electronic perturbations. The solvatochromic data are supportive of a general solvent effect, which is further confirmed by Lippert–Mataga correlation. End-capping with butterfly shaped phenothiazine restrained the formation of molecular aggregates in the solid state. All of the compounds displayed exceptional thermal stability attributable to the rigid carbazole building block. Solution processed OLED fabricated using the new materials as emitting dopants in 4,4'-bis(9*H*-carbazol-9-yl)biphenyl host exhibited bluish green electroluminescence.



INTRODUCTION

The development of π -conjugated organic materials had drawn immense attention from the scientific community due to their unique optical and electronic properties. During the past two decades, functional materials suitable for application in organic light-emitting diodes (OLEDs) based on small molecules,^{1,2} dendrimers,³ and polymers⁴ have been actively investigated. Among them, small molecules are attractive due to their well-defined molecular structure, precise control on functional properties of the materials, ability to deliver unachievable purity by polymers, and capability to be processed in solution and vacuum deposition methods.² Current focus on OLED research is mainly on device optimization methods, development of pure color emitters (red, green, and blue) suitable for solution processable devices, thermal stability, and triplet harvesting strategies such as thermally assisted delayed fluorescence.^{5,6} Thus, the development of π -conjugated small molecules and establishment of their structure–property relationships are desirable.^{7,8} In this regard, the choice of building blocks should be examined carefully, because they tend to dominate the functional properties of the materials.^{8,9} Also, the topological arrangements of the functional units around the central building block influence greatly the physicochemical, thermal, and carrier transport properties.^{6,9–13} Nevertheless, the system-

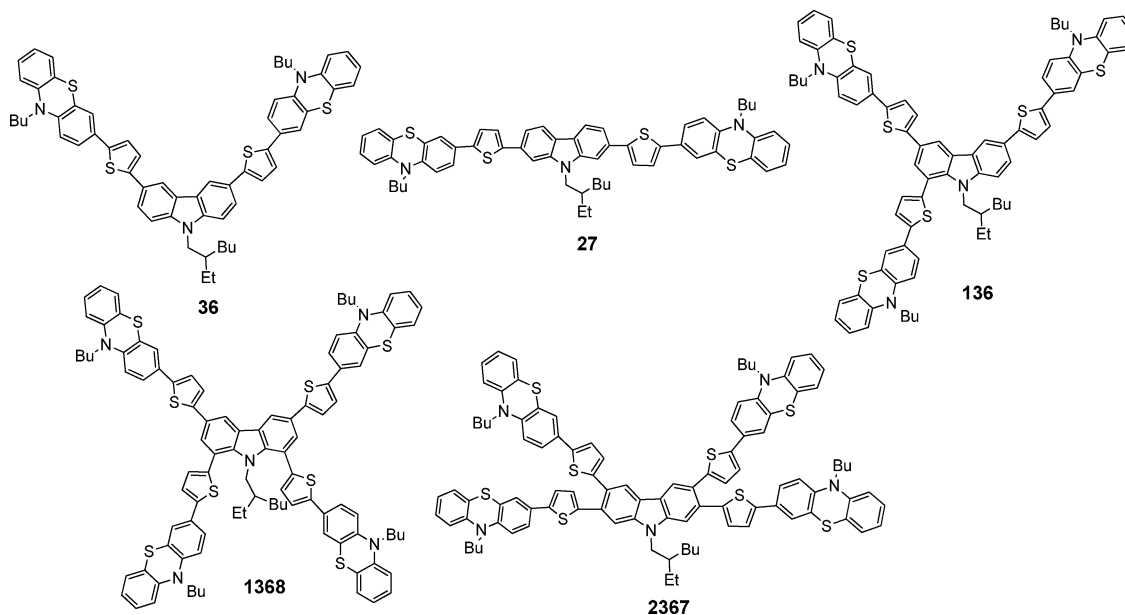
atic studies on the π -conjugated oligomers and their linking topology effects on materials properties deserve more attention. Recently, it has been found that construction of molecular materials with multifunctional building blocks is considered as a promising strategy to improve the performance characteristics of light-emitting devices.¹⁴

In this work, we have chosen to develop materials integrating carbazole and phenothiazine. Among the heterocyclic compounds, 9*H*-carbazole is one of the prototypical molecules and is adopted as a promising building block for many functional organic materials due to their rigid molecular structure, availability, amorphous nature, excellent hole transporting ability, wide scope for functionality, and high thermal and photochemical stabilities.¹⁵ Apart from these interesting features, its high triplet energy (2.9 eV) makes it a suitable host for phosphorescent OLEDs (PhOLEDs).^{16,17} To date, carbazole and its derivatives are successfully applied in OLEDs,^{9–13,16,17} organic thin film transistors (OFETs),¹⁸ photovoltaic cells,^{19,20} photorefractive materials,²¹ and as receptors in fluorescent sensors.²² Structurally, phenothiazine can be considered as sulfur inserted carbazole.²³ Its unique

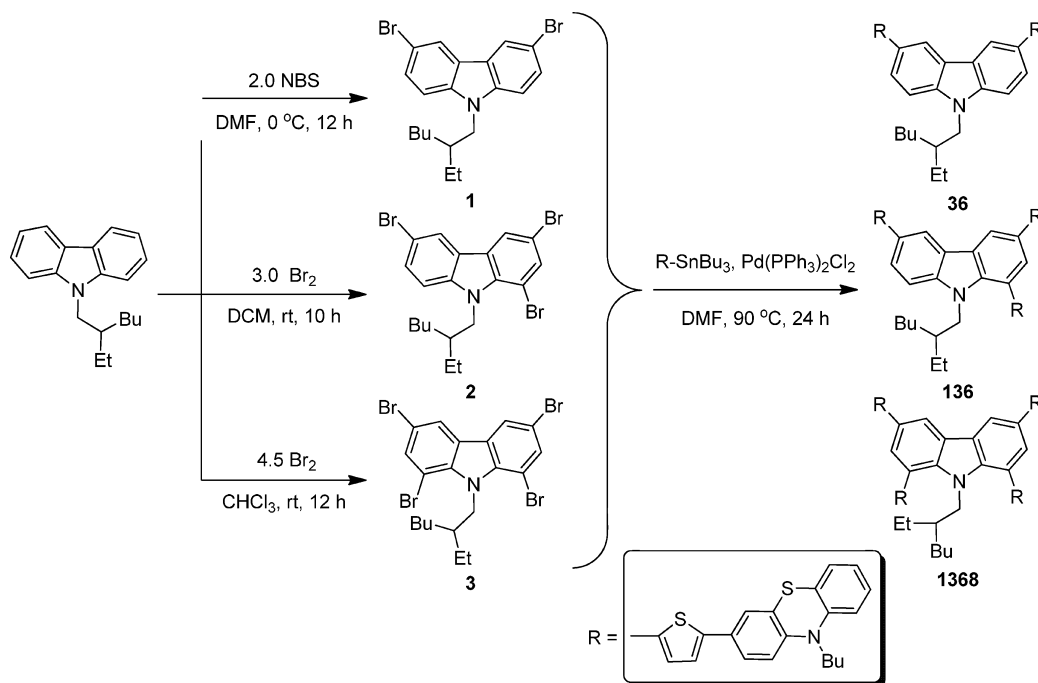
Received: April 9, 2015

Published: May 7, 2015

Chart 1. Structures of the Compounds



Scheme 1. Synthetic Protocol for the Di-(3,6)-, Tri-(1,3,6)-, and Tetra-(1,3,6,8)-Substituted Derivatives



butterfly configuration and high electron-rich character are beneficial for its potential function in optoelectronic applications.^{24–28} Recently, Jiang and co-workers reported a potential host material for PhOLEDs by connecting phenothiazine and carbazole by C–N linkage.²⁵ As a result of the large dihedral angle between carbazole and phenothiazine, the material inherited high thermal stability and aggregation free solid film. Also, the reasonably high HOMO (–5.37 eV) energy level suggests that incorporation of electron-rich phenothiazine onto carbazole would be beneficial to increase the hole mobility. Although the structure–property relationships of fluorene, pyrene, triphenylamine, and carbazole-functionalized carbazoles were well documented in the literature,^{5,9–13} systematic studies on structure–function correlation for

carbazole-phenothiazine conjugates remained unexplored. We envisaged that introduction of nonplanar phenothiazine as an end-capping unit into carbazole building block with different linking topology would be beneficial to improve the functional properties such as thermal stability, inhibition toward formation of molecular aggregates in solid film, amorphous nature, and charge carrier mobility.

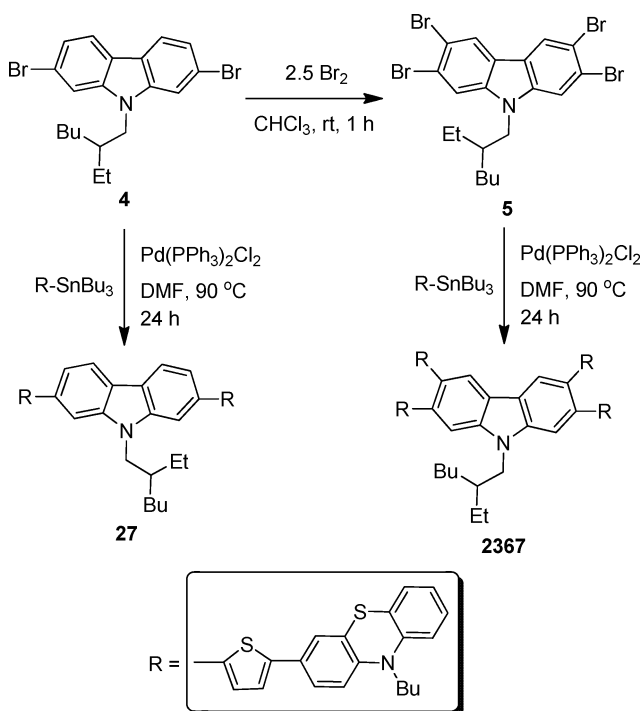
Halogenation of aromatics and heteroaromatics and metal-catalyzed cross-coupling reactions (Suzuki, Stille, Sonogashira, Buchwald–Hartwig, etc.) are the two fundamental protocols often used to access library of functional materials. Carbazole can be easily functionalized on 1, 2, 3, 6, 7, and N positions. Although the vast amount of carbazole-based materials are derived from trifunctionalization (2, 7, and N or 3, 6, and N),

few compounds containing chromophores on 1,8 positions are also known.^{15–22} However, tri- (1,3,6) and tetra-substituted (1,3,6,8 and 2,3,6,7) derivatives are less explored. In this Article, we describe carbazole-phenothiazine conjugates representing a different number of phenothiazine loading on the carbazole nucleus. Di-, tri-, and tetra-substituted carbazole derivatives (Chart 1) were synthesized to study the effect of thienylphenothiazine chromophore loading on carbazole nucleus on photophysical, electrochemical, and thermal properties. To understand the electronic properties of the compounds, time-dependent density functional theory (TDDFT) computations were also performed. Introduction of phenothiazine as an end-capping unit improved thermal stability of the materials significantly and led to rich redox characteristics. The electroluminescent characteristics were evaluated in the multi-layered OLED device by employing them as cyan or green emitting dopants in CBP host.

RESULTS AND DISCUSSION

Synthesis and Characterization. Syntheses of the di-, tri-, and tetra-substituted carbazole derivatives were accomplished as illustrated in Schemes 1 and 2. Bromination of 9-(2-ethyl-

Scheme 2. Synthetic Methodology for the Di-(2,7)- and Tetra-(2,3,6,7)-Substituted Derivatives



hexyl)-9H-carbazole using 2.0, 3.0, or 4.5 equiv of bromine in DMF, DCM, or chloroform formed the 3,6-dibromo-, 1,3,6-tribromo-, and 1,3,6,8-tetrabromo-derivatives 1–3, respectively. Similarly, reaction of 2.5 equiv of bromine with 2,7-dibromo-9-(2-ethylhexyl)-9H-carbazole (4) in chloroform produced 2,3,6,7-tetrabromo-9-(2-ethylhexyl)-9H-carbazole (5) in excellent yield. Finally, Stille coupling²⁹ reaction of the bromides (1–5) with 3-(5-tributylstannanyl-thiophen-2-yl)-10H-phenothiazine gave the targeted carbazole-phenothiazine hybrids in good yields. The dyes were thoroughly characterized by ¹H and ¹³C nuclear magnetic resonance (NMR) spectroscopy and high-resolution mass spectroscopy (HRMS). All of the

molecules inherited yellow color and are reasonably soluble in common organic solvents such as dichloromethane (DCM), toluene (TOL), chloroform (CHCl₃), tetrahydrofuran (THF), and *N,N*-dimethylformamide (DMF), but insoluble in alcohols.

Photophysical Properties. Optical properties of the compounds were evaluated by measuring absorption and emission spectra in dichloromethane. The absorption spectra of the dyes are displayed in Figure 1a, and the pertinent data are collected in Table 1.

All of the dyes displayed two distinguishable absorption bands. The higher energy absorption band at ca. 334–311 nm is assigned to the localized π - π^* electron transitions originating from the thienylphenothiazine chromophore or carbazole core. The lower energy absorption peak ca. 382–415 nm stems from the delocalized π - π^* electronic transitions from the conjugation segment comprising carbazole, thiophene, and phenothiazine units. Interestingly, the dye 27 exhibited the most red-shifted absorption maxima (415 nm) in the series attributable to the higher degree of linear conjugation offered by the chromophores in the 2,7-positions of carbazole than those in 1, 3, 6, and 8 positions (36, 136, and 1368).^{9,20,30} Anomalous behavior is rationalized by comparing the dihedral angles between the carbazole and phenothiazine chromophores at C2 and C7 in the optimized molecules. The dihedral angle between the carbazole and thiophene units (Figure 2) is significantly larger (>50°) for 2367 than for 27 (25.7°). The larger twisting would jeopardize the interchromophoric electronic communication and reduce the electronic delocalization extent. Thus, the conjugation pathway along the C2–C7 axis is perturbed in 2367 due to the additional substitution via C3 and C6. Similarly, planarity between the carbazole and thiophene units at C3 and C6 is affected on further introduction of substituents at C2 and C7 positions (compare 36 and 2367). On the other hand, although the substitution at C1 and C8 positions does not affect the coplanar arrangement of carbazole and thiophenes at C3 and C6 positions (compare 36, 136, and 1368), the chromophores at these positions (C1 and/or C8) twisted out of the plane as a result of the large dihedral angle (61.3°). Therefore, the electronic communication between the chromophores at these positions (C1 and/or C8) and the central carbazole unit is not very strong in the ground state. These results suggest that the conjugation in 136 and 1368 is limited to substituents in C3 and C6, which resulted in similar absorption spectral profiles for these derivatives.^{5,9,11–13} Among the tetra-substituted carbazole derivatives, 2367 exhibited intense absorption attributable to the orbital interaction of thienylphenothiazine segments at C2 and C7 via the carbazole core. Thus, dye 2367, having two thienylphenothiazine units at C2 and C7, gives a more intense absorption than dyes 1368 and 36 unsubstituted at C2 and C7. The effect of phenothiazine on the absorption spectra is evident on comparing the data observed for 27 and 36 with that of the known compounds containing thiophene only. Compounds 27 and 36 exhibited a >40 nm bathochromic shift when compared to 9-ethyl-2,7-di(thiophen-2-yl)-9H-carbazole and 9-ethyl-3,6-di(thiophen-2-yl)-9H-carbazole, respectively.⁸ This indicates that the end-capping by phenothiazine is beneficial for shifting the absorption to the longer wavelength region attributable to the extension of π -conjugation by phenothiazine unit.

It is interesting to compare the absorption profiles of 136 and 1368 with the known tri- and tetra-substituted featuring

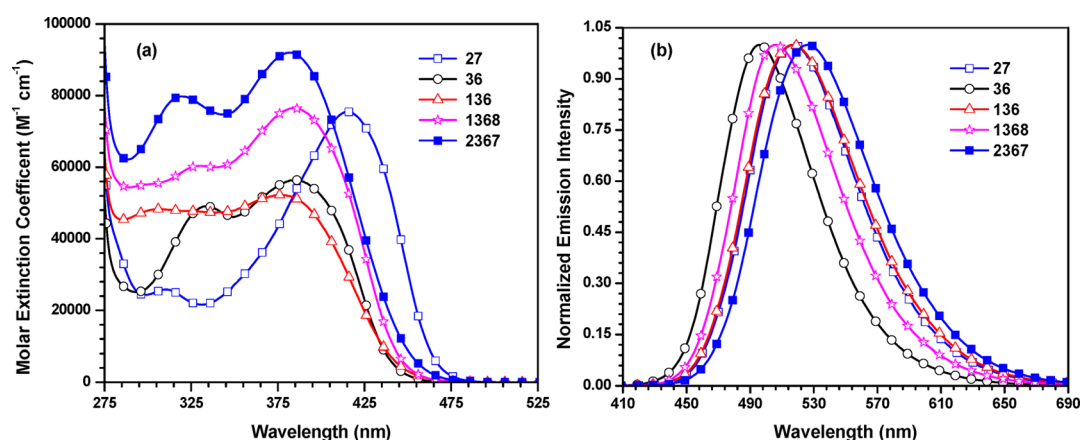


Figure 1. (a) Absorption and (b) emission spectra of the compounds recorded in dichloromethane.

Table 1. Optical Properties of the Dyes

dye	(ϵ_{\max})	λ_{\max} nm $(M^{-1} \text{cm}^{-1} \times 10^{-3})^a$	λ_{emv} nm $(\Phi_F)^{a,b}$	Stokes shift, cm^{-1}	λ_{emv}^c nm
27	415 (71.7), 311 (24.5)	518 (0.16)	4791	504	
36	385 (53.5), 334 (46.6)	496 (0.12)	5813	494	
136	375 (52.2), 307 (48.3)	517 (0.13)	7324	505	
1368	382 (74.8), 324 (58.5)	505 (0.18)	6376	502	
2367	382 (92.0), 315 (79.0)	526 (0.10)	7167	513	

^aMeasured for DCM solution. ^bAbsolute quantum yields determined by a calibrated integrated sphere system in DCM. ^cMeasured for spin-cast film.

pyrene, fluorene, carbazole, and triphenylamine peripheral chromophores.^{5,9,11,12} Because of the extension of conjugation by the thienylphenothiazine segments, the absorption maximum of compounds 136 and 1368 is red-shifted with respect to that of the later compounds. The absorption profiles of the dyes were examined in different solvents by varying the Reichardt polarity index ($E_T(30)$),³¹ cyclohexane (CH), toluene (TOL), tetrahydrofuran (THF), dichloromethane (DCM), chloroform (CHCl_3), and *N,N*-dimethylformamide (DMF). Corresponding spectra are shown in Figure 3a and

Supporting Information Figures S1–S4, and relevant data are listed in Supporting Information Table S1. They indicate that the ground state of the dyes is relatively nonpolar and devoid of significant solvent effects.

The dyes are emitting in the cyan to green region on exposure to the visible light with featureless fluorescence spectra as shown in Figure 1b. The relevant data are collected in Table 1. In contrast to the absorption trend, the emission maximum is shifted to longer wavelengths in the order $2367 > 27 > 136 > 1368 > 36$, suggesting a redistribution of electron density in the excited state. The dye 2367 exhibits the most red-shifted emission profile when compared to its congeners. This could be due to the efficient interaction of 3,6-arms with the central carbazole at the excited state. It is speculated that the molecules assume a more planar structure in the excited state. This is further confirmed by the large Stokes shifts observed for the dyes, which fell in the range $7324\text{--}4791 \text{ cm}^{-1}$. Large Stokes shifts for the fluorophores generally suggest a significant structural reorganization or polarized excited state as compared to that of ground state. The higher Stokes shift for the dyes 136, 1368, and 2367 as compared to 27 and 36 can be attributed to larger structural reorganizations in the excited state for the former compounds due to a sterically congested

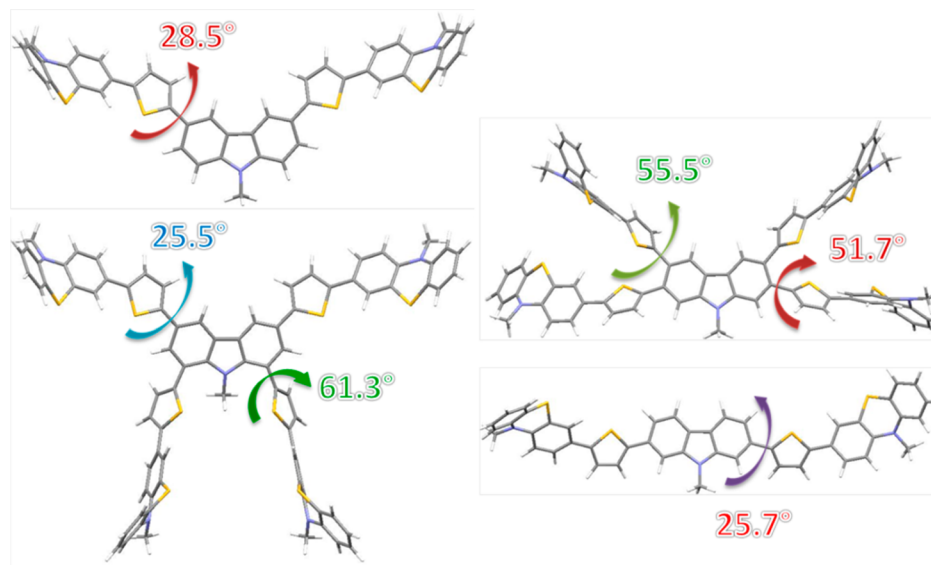


Figure 2. Variation of dihedral angles in the B3LYP/6-31G(d,p) optimized geometries of 36, 27, 1368, and 2367.

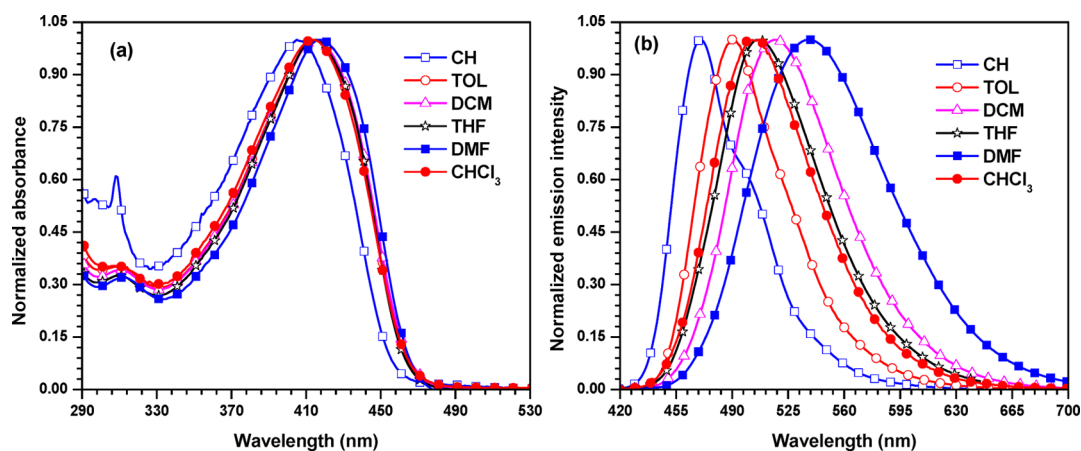


Figure 3. (a) Absorption and (b) emission spectra of the dye 27 recorded in different solvents.

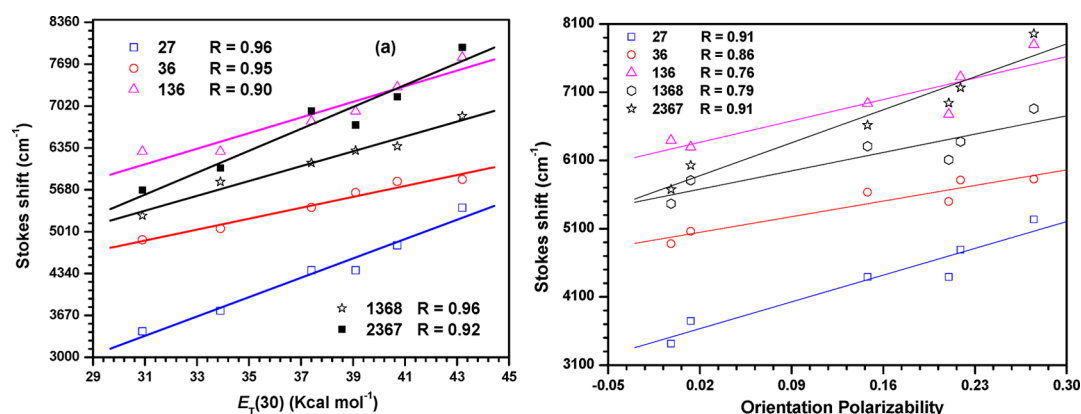


Figure 4. (a) Stokes shift versus $E_T(30)$ and (b) Lippert–Mataga plots for the dyes.

molecular structure. It is to be noted here that the reasonably large Stokes shifts is beneficial for their application in electroluminescent devices, which may help to avoid unwanted self-absorptions.^{17,32}

To investigate the impact of solvent polarity on the nature of excited state of the dyes, emission profiles (Figure 3b and Supporting Information Figures S1–S4) of the dyes were examined in solvents with different Reichardt polarity index ($E_T(30)$). The emission characteristics are highly sensitive to the solvent polarity, exhibiting a general positive solvatochromism. For instance, emission spectra recorded for the dye 27 in different solvents are displayed in Figure 3b. The moderate emission shift witnessed for the dyes on moving from CH to DMF is interesting. As the dyes do not possess a trivial donor–acceptor molecular configuration, the observed solvent-induced emission wavelength shift cannot be rationalized by considering charge-transfer excitation. It is probable that the structural reorganization for the dyes induced by photoexcitation is appreciable. Particularly, the molecular structural perturbations are more pronounced in polar solvents. It is also arguable that the excitation-induced dipole of the molecules is stabilized by interaction with the solvent dipoles. It has been observed in selected systems the incorporation of electron-rich chromophore on C2 and C7 of carbazole induces a push–pull architecture due to the difference in electron density between the chromophores.³³ Among the dyes, 2367 exhibited significant solvent-induced alternations in the emission spectra ($\Delta\lambda = 75$ nm). The difference in Stokes shift for the compounds between the nonpolar (CH) and polar solvent

(DMF) can be considered as the estimate of charge transfer character in dipolar compounds.³⁴ This assumes the following order, $2367 > 27 > 1368 > 136 > 36$, and suggests decent charge migration in the excited state for the compounds bearing substitutions in C2 and C7.

The solvatochromic data of the dyes were also examined by Lippert–Mataga and Stokes shift versus $E_T(30)$ correlations. A linear trend (Figure 4) observed for the dyes indicates a general solvent effect for them in the excited state. The change ($\Delta\mu = \mu_e - \mu_g$) in dipole moment, estimated from the plots,^{35,36} is more positive (Table 2) and suggestive of a large dipole moment for the molecules in the excited state. This is a favorable condition for the presence of weak charge transfer in these molecules. Among the dyes, 27 and 2367 exhibit a large change in dipole moment ($\Delta\mu$) confirming the more pronounced ICT for these molecules in the excited state.

Table 2. Excited- and Ground-State Dipole Moments Calculated by Different Methods^{35,36}

dye	μ_g (D) ^a	μ_e (D)			ν_{\max} vs Δf
		Lippert–Mataga	Reichardt	Kawski	
27	5.61	38.66	22.80	16.71	39.04
36	3.20	23.26	13.61	7.38	26.24
136	3.95	28.10	16.57	10.41	30.55
1368	5.24	27.91	17.70	12.60	30.74
2367	2.30	37.45	19.85	12.77	38.29

^aEstimated from the B3LYP/6-31G(d,p) calculations.

The quantum yield of the dyes decreases on increasing the solvent polarity (Supporting Information Table S2), which is suggestive of charge transfer excited state in these molecules. Also, the emission profile broadened on moving from nonpolar CH to the polar DMF. This probably supports the speculation that the initially formed Franck–Condon state or local excited state transforms into the more polar charge transfer state, which is stabilized by the polar solvents.³⁵

The emission spectra of the dyes recorded as the drop-cast thin film are displayed in Figure 5. The emission maxima of the

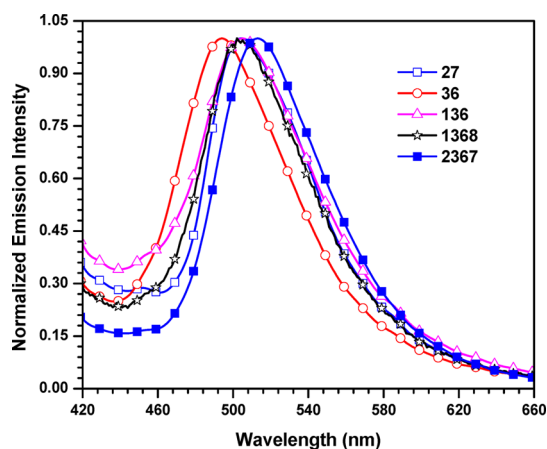


Figure 5. Emission spectra of the drop-cast thin films of the dyes.

dyes match with those observed for the tetrahydrofuran solutions (Table 1). This indicates that the dielectric constants of the thin films are close to those of tetrahydrofuran solutions. The absence of an anomalous red-shifted emission peak/shoulder for these compounds shows the beneficial role of butterfly shaped phenothiazine chromophore in retarding the formation of molecular aggregates in the solid state.

Electrochemical Properties. To ascertain the redox propensity of the dyes, cyclic voltammetric measurements were performed for the dyes in dichloromethane. The representative cyclic voltammograms recorded at a 100 mV/s scan rate are displayed in Figure 6, and the relevant data are collected in Table 3. All dyes exhibited a quasi-reversible oxidation process at more positive potentials than that observed

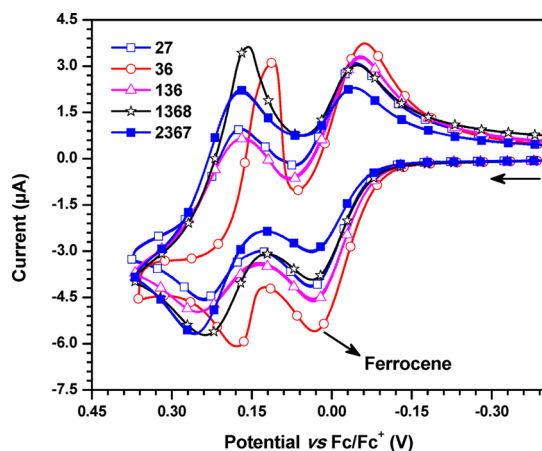


Figure 6. Cyclic voltammograms recorded for the dyes in dichloromethane (conditions: $\sim 1 \times 10^{-4}$ M solutions; scan rate, 100 mV/s; electrolyte, tetrabutylammonium perchlorate).

for ferrocene under the same conditions, attributable to the removal of electron from the thienylphenothiazine arm. Generally, the dyes possess low oxidation potentials attesting the electron-richness of the phenothiazine unit. The auxiliary effect of carbazole on the phenothiazine oxidation capability is understandable on comparing the different positional substitutions. The dye-containing 3,6-disubstitution (36) exhibited the lowest oxidation potential among the compounds. It points to the effective conjugation between the carbazole nitrogen and the thienylphenothiazine arms through the C3 and C6 positions. Yet, introduction of additional groups at C1 and C8 or C2 and C7 positions led to the increment in oxidation potential. The increase is more for C2 and C7 substitution (2367). This suggests the molecular twisting due to the additional chromophore loading, which affects the conjugation for C3 and C6 substitutions. Because the arms present in C2 and C7 are closer to C3 and C6, they led to more severe distortions in the structure (see above). Although the C2- and C7-substituted derivatives display elongated rod-like conjugation, the involvement of nitrogen electrons in the delocalization is less favored due to *meta*-like linkage with respect to nitrogen. So the 2,7-disubstituted carbazoles generally show higher oxidation potentials than the analogous 3,6-disubstituted carbazoles.^{8,9} Further, the effect of phenothiazine end-capping on oxidation potentials of the dyes is evident on comparing the data observed for 27 and 36 with those of the thiophene-substituted carbazoles.⁸ The new dyes exhibited low positive oxidation potentials when compared to the thienylcarbazoles.⁸ Also, it is interesting to compare the electrochemical behavior of 27 and 36 with 5,5'-bis(10-hexyl-10H-phenothiazin-3-yl)-2,2'-bithiophene.²⁶ Insertion of carbazole between the two thienylphenothiazine units of the later with different linking topology improved the oxidation propensity significantly.

The HOMO energies of the compounds were estimated by using the first oxidation potential and fall in the range 4.95–5.02 eV. The LUMO energy values were calculated by subtracting the optical band gap (E_{0-0}) from the HOMO energy. The E_{0-0} value was determined from the intersection of absorption and emission spectra. Generally, the HOMO and LUMO energies of the materials are sensitive to the electron-donating and -withdrawing segments attached to the π -electronic system, respectively. The incorporation of electron-donating units normally raises the HOMO energy level. Yet, in the present series of compounds, an anomalous trend was observed. Interestingly, the HOMO of the tri- (136) and tetra-substituted (1368 and 2367) dyes is lower in energy than that of the disubstituted derivative 36. This is mainly due to the steric crowding-induced electronic deconjugation in the molecule. Similar observations have been made earlier for 1,3,6,8- and 1,3,6-substituted carbazole derivatives.^{5,9,11–13}

Thermal Properties. Thermal stability of the compounds was examined by thermogravimetric analysis (TGA) under N_2 atmosphere at a heating rate of 10 °C/min. All dyes exhibited excellent thermal stability with high thermal decomposition temperature (T_d) in the range 463–478 °C. The onset decomposition temperatures corresponding to the 10% weight loss (T_{onset}) are in the range 385–400 °C. The tetra-substituted derivatives (1368 and 2367) are markedly more thermally stable than the di- (36 and 27) and tri-substituted (136) analogues. It is noteworthy that the thermal stability of 136 and 1368 is much better than that of tetra-substituted carbazole-fluorene⁹ and comparable to that of the carbazole-pyrene and carbazole-triphenylamine conjugates.^{5,12} This suggests that the

Table 3. Thermal and Electrochemical Data of the Dyes

dye	T_{onset}^a , °C	T_d^b , °C	T_m^c , °C	E_{ox}^d , V (ΔE_p , mV) ^b	HOMO, eV ^c	LUMO, eV ^d	E_{0-0} , eV ^e
27	385	463	190	0.21 (61)	-5.01	-2.30	-2.71
36	390	464	140	0.15 (59)	-4.95	-2.11	-2.84
136	392	472	150	0.22 (70)	-5.02	-2.23	-2.79
1368	400	480	170	0.19 (60)	-4.99	-2.19	-2.80
2367	398	478	230	0.22 (70)	-5.02	-2.32	-2.70

^aTemperature corresponding to 10% weight loss. ^bMeasured for 0.1 mM dichloromethane solutions and the potentials are quoted with reference to ferrocene internal standard. ^cHOMO = $4.8 + E_{\text{ox}}$. ^dLUMO = HOMO - E_{0-0} . ^eOptical band gap obtained from the intersection of normalized absorption and emission spectra.

phenothiazine group is helpful to improve the thermal robustness of the molecules.

Theoretical Studies. To establish a correlation between the photophysical behavior and geometry of these materials, we have performed theoretical calculations using density functional theoretical methods.³⁷ To minimize the computational cost, lengthy alkyl chains were replaced with the methyl segment in the model compounds. We presumed that the replacement of alkyl chains would not affect the parameters required for the discussion here. The geometries of the model compounds were optimized under vacuum by using density functional theory (DFT) with the Becke's three-parameter functional that was hybridized with the Lee–Yang–Parr correlation functional and 6-31 G(d,p) basis set.³⁸ TDDFT computations at the same theoretical level were used to estimate the vertical excitations and their orbital contributions.

The electronic distribution in the frontier molecular orbitals of the tetra-substituted derivatives 1368 and 2367 is shown in Figure 7 and Supporting Information Figure S5. The HOMO is mainly contributed by the thienylphenothiazine arms in the C3 and C6 in the dyes 36, 136, 1368, and 2367. It is diffused into the central core except for 2367. The deconjugation of central carbazole from the thienylphenothiazine arms in C3 and C6 for

2367 is mainly caused by the steric crowding due to the substitution at C2 and C7. In 27, the HOMO is delocalized over the entire molecule. The LUMOs in the molecules are invariably constituted by the carbazole core and the thiophene linker for all of the dyes except 2367. In case of 2367, the LUMO is spread over the carbazole and thiophene segments at 2,7-positions. The well-separated arrangement of HOMO and LUMO in 2367 is indicative of the charge-transfer excited state for the HOMO to LUMO electronic transition. This may be also beneficial for the bipolar charge transport retards the reverse energy transfer in electroluminescent devices.^{17,28} HOMO-1 is restricted to the thienylphenothiazine arms in C2, C3, C6, and C7. Interestingly, the thienylphenothiazine arms in C1 and C8 did not contribute to the formation of HOMO-1. However, the LUMO+1 for the dyes 136 and 1368 are predominantly composed of the arms attached to the C1 and C8, while for the remaining compounds it is mainly on the thiophene linker. These results reveal that the substitution at C1 and/or C8 may be utilized to fine-tune the electron-accepting ability of the molecules. The energies of the HOMO and LUMO levels and HOMO–LUMO energy gap values computed for the dyes (27, 36, 136, 1368, and 2367) are listed in Supporting Information Table S3. The computed HOMO and LUMO energy levels fall in the narrow ranges of 4.70–4.79 and 1.19–1.54 eV, respectively. The band gap (HOMO–LUMO) of the dyes is in the range of 3.23–3.55 eV. The LUMO energies and the energy gap calculated for the dyes in the gas phase significantly deviated from the values deduced from electrochemical and optical measurements, respectively, which probably indicate a role of solvent interaction with the molecules.

The computed energies of the vertical excitations and their oscillator strengths and orbital contributions are listed in Supporting Information Table S3. The calculated lowest energy vertical transition for the compounds in the vacuum phase is in agreement with the experimentally observed results for the dyes in dichloromethane solution. This observation further supports the absence of a significant solvent polarity effect on the ground state, which corroborates the solvent insensitive absorption spectra recorded for the compounds.

To evaluate the charge carrier mobility (hole and electron) of these materials, internal reorganization energies for the electron (λ_-) and hole (λ_+) were calculated theoretically at the B3LYP/6-31G(d,p) level. According to the Marcus–Hush equation,³⁹ the charge-transfer rate mainly depends on two key parameters such as reorganization energy ($\lambda_{h/e}$) and electronic coupling matrix (V).

$$K_{\text{hole/electron}} = \left[\frac{4\pi^2}{h} \right] \frac{1}{\sqrt{4\pi K_B T \lambda_{+/-}}} V^2 \exp \left[-\frac{\lambda_{+/-}}{4K_B T} \right]$$

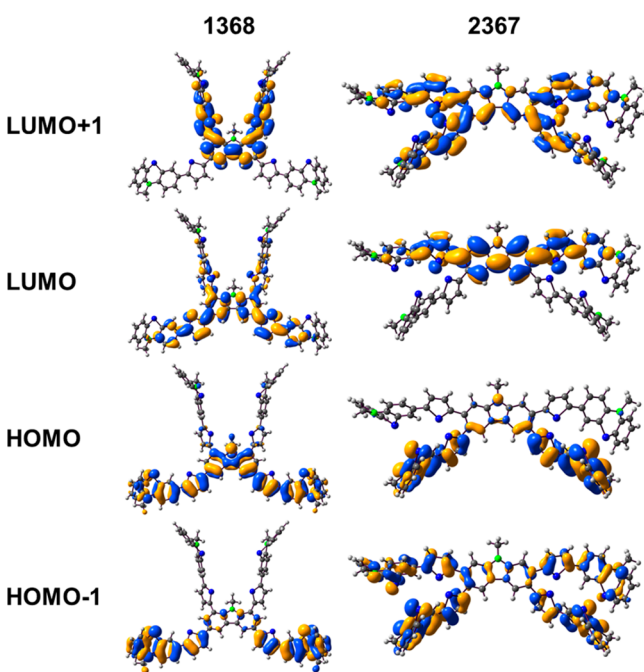


Figure 7. Frontier molecular orbitals (HOMO and LUMO) for the model compounds of 2367 and 1368 computed at the B3LYP/6-31G(d) level.

Experimentally, V values are in the narrow range, and it is tedious to determine the accurate V value in amorphous solid films because of direct contact.⁴⁰ However, charge mobility can be directly correlated with the respective reorganization energies (λ_{\pm}) of the materials, and it is inversely proportional to the charge transfer rate. Using this relation, reasonable correlation between the molecular structure and charge transfer rate in organic semiconductors has been established.⁴¹ The calculated internal reorganization energies (λ_{\pm}) of the materials are listed in Table 4. As mentioned above, small λ_{\pm} indicates

Table 4. Computed Reorganization Energies for Hole (λ_{+}) and Electron (λ_{-}), Ionization Potentials (I_p), and Electron Affinities (E_a) (All Values Are in eV) for Optimized Models of Dyes

dye	I_p^a	I_p^b	E_a^a	E_a^b	λ_{+}	λ_{-}
36	5.47	5.60	0.79	0.61	0.24	0.34
27	5.45	5.57	0.50	0.29	0.23	0.35
136	5.38	5.48	0.60	0.43	0.19	0.27
1368	5.32	5.40	0.64	0.49	0.16	0.24
2367	5.36	5.44	0.77	0.55	0.15	0.36

larger charge mobility. The hole reorganization energies (λ_{+}) decrease with increasing the phenothiazine chromophore loading on carbazole. Thus, the tetra-substituted compounds **1368** and **2367** are predicted to possess high hole mobility in the series. The ionization potentials of the compounds were in agreement with the above trend. The electron reorganization energies (λ_{-}) of the compounds are slightly larger, indicating poor electron mobility in the molecular layers.

Electroluminescence Characteristics. The electroluminescence of the compounds was examined by using them as emitting dopants in solution processed multilayered OLED devices. The device configuration is ITO/PEDOT:PSS/CBP + **36** or **27** or **136** or **1368** or **2367** (10 wt %)/TPBi/LiF/Al, where poly(3,4-ethylene-dioxythiophene)-poly(styrenesulfonate) (PEDOT:PSS) served as hole transporting layer (HTM), while 1,3,5-tris(*N*-phenylbenzimidazol-2-yl)benzene (TPBi) functioned as an electron-transport material (ETM). The organic layers were sandwiched between the ITO anode and Al cathode. An additional electron injection layer (LiF) was also used. For the doped devices, 4,4'-bis(9*H*-carbazol-9-yl)biphenyl (CBP) was used as host material. The energy level alignment for the materials used in the devices is depicted in Figure 8. From this it is understandable that the hole injection barrier at the HTM/dye interface is small (<0.1 eV) and favorable for effective hole injection. However, there is a significant barrier (<0.38 eV) for electron injection from the ETM into the dyes. This may relatively hinder the electron flow into the dye layer. Interestingly, the dyes containing substitution at C2 and C7 (**27** and **2367**) possess relatively less barrier for electron injection.

The current density versus voltage (I - V) and current density versus luminance plots (I - L) of the doped OLED devices are shown in Figure 9, and the pertinent electroluminescence parameters are listed in Table 5. The dyes containing substitution at C2 and C7 (**2367** and **27**) exhibited relatively low turn-on voltages (V_{on}) attributable to the low-lying LUMO energy level. This would facilitate the effective injection of electrons in the corresponding molecular layers. Also, they exhibited reasonably high luminance reflecting their emission characteristics and effective exciton capture from the host

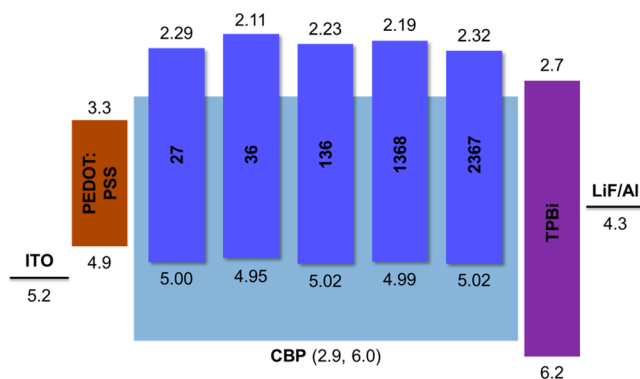


Figure 8. Energy level diagram of the OLED device that was doped with 10 wt % of **27**, **36**, **136**, **1368**, and **2367** (all values are in eV with respect to vacuum level).

matrix. In electroluminescence (EL) spectra (Figure 10), the bright green emission was observed for the devices (**27**, **136**, and **2367**) with peaks centered at 500–508 nm and Commission International de l'Éclairage coordinates (CIE) of (0.23, 0.54), (0.21, 0.46), and (0.23, 0.54). For the devices doped with **1368** and **36**, cyan emission was observed at the wavelength maxima of 484 and 492 nm, respectively, with CIE coordinates of 0.17, 0.35 and 0.19, 0.39. The EL spectra of the diodes resemble the photoluminescence (PL) spectra of the materials as thin film. These results further confirmed that the obtained electroluminescence from the doped devices is from the desired emitting layer (EML) and lack of aggregate formation in the solid state. Also, the observed EL spectra of the OLED persisted over the entire operating voltages studied. The narrow fwhm values of the electroluminescence spectra indicate the color purity of the devices. Overall, the best performance was observed for **2367** doped device with maximum luminescence and current efficiency. This may be attributed to the efficient trapping of excitons by **2367** from the CBP layer due to the favorable alignment of energy levels with the host matrix.

CONCLUSIONS

In summary, we have synthesized a new class of polysubstituted carbazoles with phenothiazine chromophore linked via a thiophene spacer as cyan or green emitters in solution processed doped OLED. The absorption spectra of the compounds are highly dependent on the substitution pattern and are insensitive to the solvent polarity. Yet, the emission spectra were significantly altered by the polarity of solvent, and the observed positive solvatochromic behavior suggests a more polar excited state involving significant structural changes. The emission characteristics such as large Stokes shift, featureless broad fluorescence, and large dipole moment change support the structural change in the excited molecule involving electronic redistribution. Lippert–Mataga and $E_T(30)$ correlations of the solvatochromic data and DFT calculation results suggest a more polar excited state for molecules **2367** and **27** than for their congeners. The tetra-substituted derivatives displayed high thermal stability in the series. Solution processed multilayered OLED were fabricated by employing **27**, **36**, **136**, **1368**, and **2367** as dopants in CBP host matrix and were found to exhibit bluish green emission. A device fabricated with **2367** exhibited superior performance in the series attributable to the well-aligned energy levels and emission characteristics. Further studies to exploit the use of these materials as hole transporting

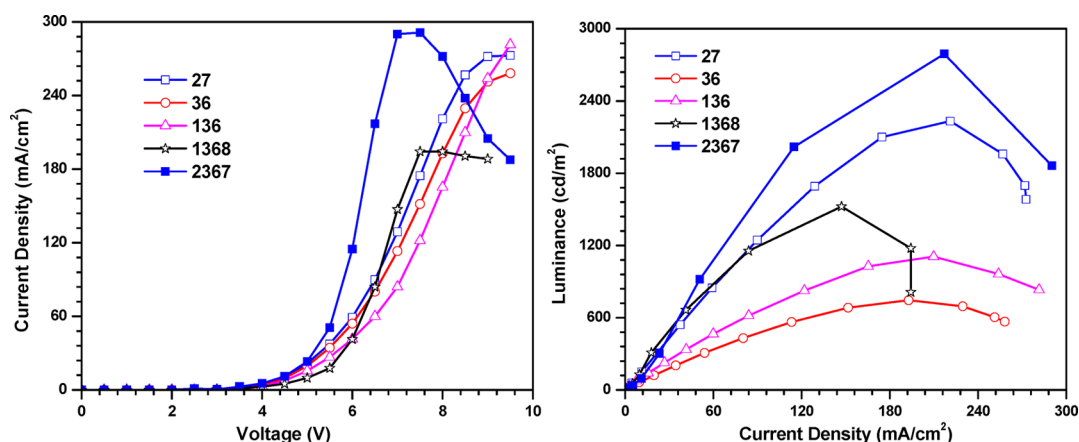


Figure 9. I – V – L characteristics of the OLEDs doped (10%) with 27, 36, 136, 1368, and 2367.

Table 5. Device Performance Characteristics of the Doped (10%) OLEDs

dye	V_{on} , V ^a	η_c , cd/A ^{b,c}	L_{max} , cd/m ²	λ_{EL} , nm	fwhm, nm	CIE (x,y) ^c
27	4.2	1.3/1.4	2233	500	81	(0.23,0.54)/(0.23,0.53)
36	4.8	0.6/–	754	484	75	(0.17,0.35)/–
136	4.7	1.0/0.6	1107	500	80	(0.21,0.46)/–
1368	4.8	1.2/1.4	1523	492	78	(0.19,0.39)/(0.19,0.42)
2367	4.5	0.9/1.8	2791	508	84	(0.23,0.52)/(0.23,0.51)

^aTurn-on voltage. ^bCurrent efficiency. ^cAt 100/1000 cd/m².

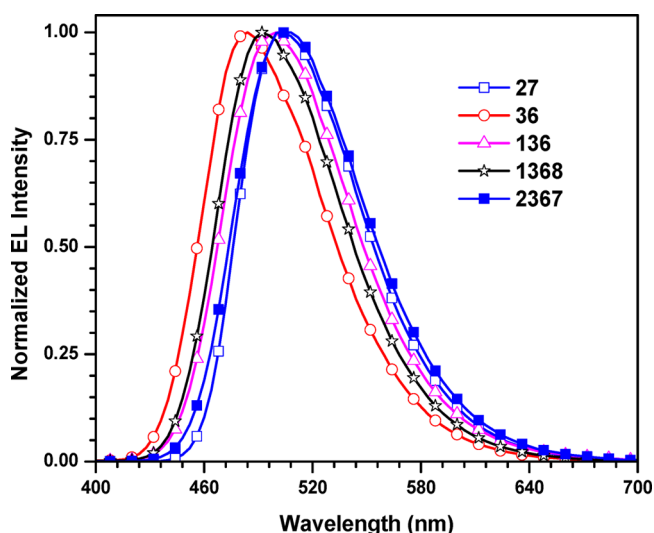


Figure 10. Electroluminescence spectra of the samples doped (10%) with 27, 36, 136, 1368, or 2367.

materials in photovoltaic devices are in progress in our laboratory.

EXPERIMENTAL SECTION

General Methods. All required precursor chemicals were obtained from commercial sources and used as received without any further purification. The solvents used for synthesis and analytical measurements were dried by following standard procedures and distilled prior to use. Column chromatography technique was performed on 100–200 mesh silica as the stationary phase in a 30 cm long and 2.0 cm diameter column. ¹H and ¹³C NMR spectral data were collected in CDCl₃ on an FT-NMR spectrometer operating at 500.13 and 125.77 or 400 and 100.00 MHz, respectively. Me₄Si (0.00 ppm) was used as internal standard to calibrate the chemical shift values. Mass spectral (HRMS) data were recorded on an ESI TOF high-resolution mass

spectrometer in positive mode. The electronic absorption and emission spectral data were collected at room temperature using a UV–vis spectrophotometer. Appropriate dilute solutions were used for the measurements, which were performed at room temperature. Absolute quantum yields were determined by a calibrated integrating sphere connected to the spectrofluorimeter. Cyclic voltammetry experiments were performed by using an electrochemical analyzer with a conventional three-electrode configuration consisting of a glassy carbon working electrode, platinum auxiliary electrode, and a nonaqueous Ag/AgNO₃ reference electrode. The $E_{1/2}$ values were determined as $(E_p^a + E_p^c)/2$, where E_p^a and E_p^c are the anodic and cathodic peak potentials, respectively. The potentials are quoted against ferrocene internal standard. Thermogravimetric analysis (TGA) was performed under nitrogen atmosphere at a heating rate of 10 °C/min.

Synthesis. The precursors **1** and **4** were synthesized according to the following literature procedure.⁴²

1,3,6-Tribromo-9-(2-ethyl-hexyl)-9H-carbazole (2). To a stirred solution of 9-(2-ethyl-hexyl)-9H-carbazole (1.00 g, 7.15 mmol) in 20 mL of dichloromethane in a 250 mL round-bottom flask was added bromine (1.10 mL, 22.16 mmol) diluted in 10 mL of dichloromethane dropwise through a dropping funnel at room temperature for 10 min. After the addition, stirring was allowed for a further 10 h at room temperature. After completion of reaction, excess of bromine was removed by washing with aqueous sodium hydrogen sulfate. The reaction mixture was extracted with DCM (2 × 20 mL), dried over anhydrous sodium sulfate, and evaporated to dryness. The resultant crude product was purified by column chromatography using hexanes as eluent to offer the title compound **2** (1.36 g, 60%) as a white color solid; mp 120–130 °C. ¹H NMR (500.13 MHz, CDCl₃, δ ppm): 8.02 (d, J = 5.0 Hz, 1H), 7.97 (d, J = 1.5 Hz, 1H), 7.69 (d, J = 2.0 Hz, 1H), 7.54–7.52 (m, 1H), 7.21 (d, J = 9.0 Hz, 1H), 4.45–4.33 (m, 2H), 2.05–2.00 (m, 1H), 1.32–1.12 (m, 8H), 0.81 (t, J = 7.0 Hz, 6H). ¹³C NMR (CDCl₃, 100.00 MHz, δ ppm): 140.7, 135.9, 133.6, 129.5, 126.1, 122.8, 122.0, 112.6, 111.7, 103.5, 48.0, 40.4, 30.2, 28.4, 23.5, 23.0, 13.9, 10.8. HRMS calcd for C₂₀H₂₂NBr₃ [M + H]⁺ m/z 514.9282, found 514.9283.

1,3,6,8-Tetrabromo-9-(2-ethylhexyl)-9H-carbazole (3). It was obtained from carbazole (1.5 g, 5.37 mmol) and bromine (1.7 mL,

26.85 mmol) by following the procedure described above for **2**, but chloroform was used as solvent. White crystalline solid; yield: 2.4 g, 76%; mp 130–140 °C. ¹H NMR (500.13 MHz, CDCl₃, δ ppm): 8.05 (d, *J* = 2 Hz, 2H), 7.77 (d, *J* = 1.5 Hz, 2H), 5.13 (d, *J* = 8 Hz, 2H), 1.85–1.81 (m, 1H), 1.10–1.00 (m, 8H), 0.74–0.69 (m, 6H). ¹³C NMR (CDCl₃, 100.00 MHz, δ ppm): 134.8, 121.9, 112.9, 105.1, 48.3, 40.0, 29.0, 27.7, 22.9, 22.2, 13.0, 10.4. HRMS calcd for C₂₀H₂₁NBr₄ [M + H]⁺ *m/z* 594.8366, found 594.8367.

2,3,6,7-Tetrabromo-9-(2-ethyl-hexyl)-9H-carbazole (5). It was obtained from 2,7-dibromo-9-(2-ethyl-hexyl)-9H-carbazole (2.0 g, 4.50 mmol) and bromine (1.0 mL, 11.25 mmol) by following the procedure described above for **2**, but chloroform was used as solvent. In the final step, a white precipitate was obtained, which was found to be analytically pure enough and so no column chromatography was required. Yield: 2.15 g, 96%; mp 118–125 °C. ¹H NMR (500.13 MHz, CDCl₃, δ ppm): 8.21 (s, 2H), 7.62 (s, 2H), 4.01 (t, *J* = 10.0 Hz, 2H), 1.99–1.94 (m, 1H), 1.36–1.24 (m, 8H), 0.92–0.87 (m, 6H). ¹³C NMR (CDCl₃, 100.00 MHz, δ ppm): 140.7, 124.7, 122.2, 122.0, 114.6, 114.0, 47.8, 39.0, 30.7, 28.4, 24.2, 22.9, 14.0, 10.8. HRMS calcd for C₂₀H₂₁NBr₄ [M + H]⁺ *m/z* 594.8366, found 594.8367.

3,3'-(5,5'-(9-(2-Ethylhexyl)-9H-carbazole-3,6-diyl)bis(thiophene-5,2-diyl)bis(10-butyl-10H-phenothiazine) (36). A mixture of **1** (0.70 g, 1.62 mmol), 10-butyl-3-(5-tributylstannanyl-thiophen-2-yl)-10H-phenothiazine (2.60 g, 4.00 mmol), and Pd(PPh₃)₂Cl₂ (1 mol %) was dissolved in 10 mL of DMF and degassed with N₂ for 15 min in a 100 mL round-bottom flask. The reaction mixture was heated at 90 °C for 24 h under N₂ atmosphere. After completion of the reaction, distilled water (40 mL) was added and extracted with DCM, dried over anhydrous sodium sulfate, and dried. The resultant crude product was purified by column chromatography using CH₂Cl₂:hexanes (1:3) as eluent to offer the desired compound **36** (0.72 g, 74%) as a yellow color solid; mp 180–190 °C. ¹H NMR (500.13 MHz, CDCl₃, δ ppm): 8.33 (d, *J* = 1.5 Hz, 2H), 7.74 (dd, *J* = 1.5, 5.0 Hz, 2H), 7.43–7.42 (m, 4H), 7.37 (d, *J* = 8.0 Hz, 2H), 7.30 (d, *J* = 3.5 Hz, 2H), 7.20 (d, *J* = 3.5 Hz, 2H), 7.17–7.15 (m, 4H), 6.94–6.85 (m, 6H), 4.17–4.12 (m, 2H), 3.87 (t, *J* = 6.5 Hz, 4H), 2.07–2.04 (m, 1H), 1.83–1.79 (m, 4H), 1.52–1.27 (m, 9H), 0.98–0.86 (m, 15H). ¹³C NMR (CDCl₃, 125.77 MHz, δ ppm): 140.8, 127.3, 125.8, 124.5, 124.0, 123.1, 122.9, 122.5, 117.4, 115.4, 109.4, 47.5, 39.5, 31.7, 31.0, 28.8, 27.0, 24.4, 23.1, 22.7, 20.2, 14.2, 13.9, 11.0. HRMS calcd for C₆₀H₅₉N₃S₄Na [M + Na]⁺ *m/z* 972.3489, found 972.3480.

3,3'-(5,5'-(9-(2-Ethylhexyl)-9H-carbazole-2,7-diyl)bis(thiophene-5,2-diyl)bis(10-butyl-10H-phenothiazine) (27). Compound **27** was synthesized from **4** (1.00 g, 2.29 mmol) and 10-butyl-3-(5-tributylstannanyl-thiophen-2-yl)-10H-phenothiazine (3.80 g, 6.87 mmol) by following a procedure similar to that described above for **36**. Pale yellow solid; yield: 1.57 g, 70%; mp 130–140 °C. ¹H NMR (500.13 MHz, CDCl₃, δ ppm): 8.03 (d, *J* = 8.0 Hz, 2H), 7.56 (s, 2H), 7.51–7.49 (m, 2H), 7.42–7.41 (m, 4H), 7.34 (d, *J* = 3.5 Hz, 2H), 7.20 (d, *J* = 4.0 Hz, 2H), 7.16 (d, *J* = 7.5 Hz, 4H), 6.94–6.91 (m, 2H), 6.88–6.84 (m, 4H), 4.21–4.17 (m, 2H), 3.87 (t, *J* = 5.0 Hz, 4H), 2.13–2.08 (m, 1H), 1.81 (t, *J* = 10.0 Hz, 4H), 1.50–1.40 (m, 9H), 0.99–0.85 (m, 15H). ¹³C NMR (CDCl₃, 125.77 MHz, δ ppm): 144.9, 144.5, 144.0, 142.4, 141.9, 132.0, 128.9, 127.5, 127.3, 125.3, 124.5, 124.3, 123.9, 123.2, 122.5, 122.1, 120.6, 117.3, 115.5, 115.4, 105.8, 47.2, 39.4, 31.0, 28.9, 26.9, 24.6, 23.1, 20.2, 13.9, 11.0; HRMS calcd for C₆₀H₅₉N₃S₄Na [M + Na]⁺ *m/z* 972.3489, found 972.3486.

3,3',3''-(5,5',5''-(9-(2-Ethylhexyl)-9H-carbazole-1,3,6-triyl)tris(thiophene-5,2-diyl)tris(10-butyl-10H-phenothiazine) (136). Compound **136** was synthesized from **2** (0.70 g, 1.36 mmol) and 10-butyl-3-(5-tributylstannanyl-thiophen-2-yl)-10H-phenothiazine (3.09 g, 4.76 mmol) by following the procedure described above for **36**. Dark-yellow solid; yield: 1.04 g, 60%; mp 220–230 °C. ¹H NMR (400.0 MHz, CDCl₃, δ ppm): 8.25 (s, 1H), 7.54 (d, *J* = 12.0 Hz, 1H), 7.41 (d, *J* = 8.0 Hz, 4H), 7.28–7.27 (m, 2H), 7.17–7.06 (m, 10 Hz), 7.05 (s, 2H), 6.88–6.86 (m, 12H), 4.11 (d, *J* = 4.0 Hz, 6H), 3.92 (t, *J* = 16 Hz, 2H), 1.80 (d, *J* = 4 Hz, 8H), 1.50–1.44 (m, 7H), 0.98–0.93 (m, 15H), 0.66 (t, *J* = 8.0 Hz, 3H), 0.56 (t, *J* = 4.0 Hz, 3H). ¹³C NMR (CDCl₃, 100.0 MHz, δ ppm): 140.7, 136.0, 133.6, 129.6, 127.9, 127.3, 126.2, 124.8, 122.8, 122.7, 122.1, 115.7, 112.6, 103.6, 48.1, 40.4, 30.2, 28.4,

23.5, 23.0, 20.1, 13.9, 13.8, 11.0. HRMS calcd for C₈₀H₇₆N₄S₆Na [M + Na]⁺ *m/z* 1307.4289, found 1307.4292.

3,3',3''-(5,5',5''-(9-(2-Ethylhexyl)-9H-carbazole-1,3,6,8-tetrayl)tetrakis(thiophene-5,2-diyl)tetrakis(10-butyl-10H-phenothiazine) (1368). Compound **1368** was prepared from **3** (0.80 g, 1.34 mmol) and 10-butyl-3-(5-tributylstannanyl-thiophen-2-yl)-10H-phenothiazine (4.50 g, 6.70 mmol) by following the procedure of **36**. Yellow solid; yield: 1.7 g, 60%; mp 165–175 °C. ¹H NMR (500.13 MHz, CDCl₃, δ ppm): 8.34 (d, *J* = 2.0 Hz, 2H), 7.74 (s, 2H), 7.44–7.42 (m, 8H), 7.37 (d, *J* = 4.0 Hz, 2H), 7.23 (d, *J* = 3.5 Hz, 2H), 7.16–7.14 (m, 10H), 6.94–6.86 (m, 14H), 3.88 (t, *J* = 7.0 Hz, 10H), 1.82–1.79 (m, 9H), 1.51–1.42 (m, 10H), 0.98–0.94 (m, 15H), 0.51 (t, *J* = 7.5 Hz, 4H), 0.27 (t, *J* = 7.0 Hz, 5H). ¹³C NMR (CDCl₃, 125.77 MHz, δ ppm): 145.0, 144.9, 144.7, 144.4, 143.8, 143.1, 141.9, 141.2, 139.3, 129.0, 128.7, 128.6, 127.6, 127.5, 127.3, 127.0, 126.4, 125.4, 125.3, 125.1, 124.8, 124.5, 124.2, 123.4, 123.1, 122.5, 122.3, 120.5, 116.8, 115.5, 115.4, 115.3, 47.2, 39.0, 34.7, 31.6, 29.0, 27.3, 26.9, 25.3, 22.7, 22.5, 20.7, 20.2, 14.1, 13.9, 11.5, 9.8. HRMS calcd for C₁₀₀H₉₃N₅S₈Na [M + Na]⁺ *m/z* 1643.5128, found 1643.5115.

3,3',3''-(5,5',5''-(9-(2-Ethylhexyl)-9H-carbazole-2,3,6,7-tetrayl)tetrakis(thiophene-5,2-diyl)tetrakis(10-butyl-10H-phenothiazine) (2367). Compound **2367** was synthesized from **5** (1.00 g, 1.68 mmol) and 10-butyl-3-(5-tributylstannanyl-thiophen-2-yl)-10H-phenothiazine (5.40 g, 7.56 mmol) by following the method described earlier for **36**. Yellow solid; yield: 1.6 g, 60%; mp 150–160 °C. ¹H NMR (500.13 MHz, CDCl₃, δ ppm): 8.19 (s, 2H), 7.51 (s, 2H), 7.36–7.34 (m, 8H), 7.16–7.11 (m, 8H), 7.09–7.08 (m, 4H), 6.91–6.81 (m, 16H), 4.22–4.16 (m, 2H), 3.86–3.82 (m, 8H), 2.13 (t, *J* = 10.0 Hz, 1H), 1.80–1.76 (m, 8H), 1.48–1.43 (m, 14H), 0.98–0.86 (m, 20H). ¹³C NMR (CDCl₃, 100.00 MHz, δ ppm): 144.8, 144.4, 143.4, 140.6, 128.7, 127.9, 127.4, 127.2, 125.1, 124.8, 124.7, 124.5, 124.0, 123.9, 122.3, 122.0, 121.9, 115.3, 115.2, 114.5, 113.9, 47.5, 47.0, 38.9, 30.5, 28.8, 28.3, 24.1, 22.9, 20.0, 14.0, 13.8, 10.7. HRMS calcd for C₁₀₀H₉₃N₅S₈Na [M + Na]⁺ *m/z* 1643.5126, found 1643.5143.

OLED Fabrication and Characterization. The OLED devices were fabricated on a precleaned glass substrate containing ITO (thickness: 125 nm) as anode, poly(3,4-ethylene-dioxythiophene)-poly(styrenesulfonate) (PEDOT:PSS, thickness: 35 nm) as a hole-injection layer (HIL), an emissive layer (EML), TPBI as an electron-transport layer (ETL) (thickness: 35 nm), a LiF electron-injection layer (EIL, thickness: 0.7 nm), and an Al layer (thickness: 150 nm) as a cathode. The aqueous solution of PEDOT:PSS was spin-coated at 4000 rpm for 20 s to form a 35 nm HIL layer. The dyes **27**, **36**, **136**, **1368**, and **2367** doped in 4,4'-bis(9H-carbazol-9-yl)biphenyl (CBP) were deposited by spin-coating at 2500 rpm for 20 s and served as emissive layer. The TPBI layer then was deposited onto it. Finally, lithium fluoride and aluminum cathode were thermally evaporated at 1.0 × 10⁻⁵ Torr.

■ ASSOCIATED CONTENT

📄 Supporting Information

Copies of ¹H and ¹³C NMR spectra, solvatochromic plots, and Cartesian coordinates of the optimized structures. The Supporting Information is available free of charge on the ACS Publications website at DOI: 10.1021/acs.joc.5b00787.

■ AUTHOR INFORMATION

✉ Corresponding Author

*krjt8fcy@iitr.ac.in

Notes

The authors declare no competing financial interest.

■ ACKNOWLEDGMENTS

K.R.J.T. is thankful to DST, New Delhi, for financial support (ref. no. DST/TSG/PT/2013/09). DST is also acknowledged for a FIST grant to establish an ESI mass spectrometer at the department. Generous access to the instrumental facility at the

Department of Chemistry and Institute Instrumentation Centre is also gratefully acknowledged. R.K.K. is thankful to CSIR, New Delhi, for a Research Fellowship.

REFERENCES

- (1) (a) Tang, C. W.; VanSlyke, S. A. *Appl. Phys. Lett.* **1987**, *51*, 913. (b) Duan, L.; Hou, L.; Lee, T. W.; Qiao, J.; Zhang, D.; Dong, G.; Wang, L.; Qiu, Y. *J. Mater. Chem.* **2010**, *20*, 6392. (c) Zhu, X. H.; Peng, J.; Cao, Y.; Roncali, J. *Chem. Soc. Rev.* **2011**, *40*, 3509. (d) Zhu, M.; Yang, C. *Chem. Soc. Rev.* **2013**, *42*, 4963. (e) Chercka, D.; Yoo, S. J.; Baumgarten, M.; Kim, J. J.; Müllen, K. *J. Mater. Chem. C* **2014**, *2*, 9083. (f) Zhan, X.; Sun, N.; Wu, Z.; Tu, J.; Yuan, L.; Tang, X.; Xie, Y.; Peng, Q.; Dong, Y.; Li, Q.; Ma, D.; Li, Z. *Chem. Mater.* **2015**, *27*, 1847.
- (2) (a) Thomas, K. R. J.; Lin, J. T.; Tao, Y. T.; Ko, C. W. *J. Am. Chem. Soc.* **2001**, *123*, 9404. (b) Thomas, K. R. J.; Lin, J. T.; Tao, Y. T.; Ko, C. W. *Chem. Mater.* **2002**, *14*, 1354. (c) Fisher, A. L.; Linton, K. E.; Kamtekar, K. T.; Pearson, C.; Bryce, M. R.; Petty, M. C. *Chem. Mater.* **2011**, *23*, 1640. (d) Krotkus, S.; Kazlauskas, K.; Miasojedovas, A.; Gruodis, A.; Tomkeviciene, A.; Grazulevicius, J. V.; Jursenas, S. *J. Phys. Chem. C* **2012**, *116*, 7561. (e) Zhang, Z.; Jiang, W.; Ban, X.; Yang, M.; Ye, S.; Bin, H.; Sun, Y. *RSC Adv.* **2015**, *5*, 29708.
- (3) (a) Thomas, K. R. J.; Velusamy, M.; Lin, J. T.; Chuen, C. H.; Tao, Y. T. *J. Mater. Chem.* **2005**, *15*, 4453. (b) Lo, S. C.; Burn, P. L. *Chem. Rev.* **2007**, *107*, 1097. (c) Burn, P. L.; Lo, S. C.; Samuel, D. W. *Adv. Mater.* **2007**, *19*, 1675. (d) Zhao, Z.; Li, J. H.; Wang, X.; Lu, P.; Yang, Y. *J. Org. Chem.* **2009**, *74*, 383. (e) Moonsin, P.; Prachumrak, N.; Namuangruk, S.; Jugsuttiwong, S.; Keawin, T.; Sudyoadsuk, T.; Promarak, V. *J. Mater. Chem. C* **2014**, *2*, 5540.
- (4) (a) Burroughes, J. H.; Bradley, D. D. C.; Brown, A. R.; Marks, R. N.; Mackay, K.; Friend, R. H.; Burns, P. L.; Holmes, A. B. *Nature* **1990**, *347*, 539. (b) Grimsdale, A. C.; Chan, K. L.; Martin, R. E.; Jokisz, P. G.; Holmes, A. B. *Chem. Rev.* **2009**, *109*, 897. (c) Gong, S.; Yang, C.; Qin, J. *Chem. Soc. Rev.* **2012**, *41*, 4797. (d) Stanislavaityte, E.; Simokaitiene, J.; Raisys, S.; Attar, H. A.; Grazulevicius, J. V.; Monkman, A. P.; Jankus, V. *J. Mater. Chem. C* **2013**, *1*, 8209.
- (5) Kotchaprastit, P.; Prachumrak, N.; Tarsang, R.; Jungsuttiwong, S.; Keawin, T.; Sudyoadsuk, T.; Promarak, V. *J. Mater. Chem. C* **2013**, *1*, 4916.
- (6) (a) Moonsin, P.; Prachumrak, N.; Namuangruk, S.; Jungsuttiwong, S.; Keawin, T.; Sudyoadsuk, T.; Promarak, V. *Chem. Commun.* **2013**, *49*, 6388. (b) Valchanov, G.; Ivanova, A.; Tadjer, A.; Chercka, D.; Baumgarten, M. *Org. Electron.* **2013**, *14*, 2727. (c) Tanaka, H.; Shizu, K.; Lee, J.; Adachi, C. *J. Phys. Chem. C* **2015**, *119*, 2948. (d) Sizu, K.; Tanaka, H.; Uejima, M.; Sato, T.; Tanaka, K.; Kaji, H.; Adachi, C. *J. Phys. Chem. C* **2015**, *119*, 1291. (e) Albrecht, K.; Matsuo, K.; Fujita, K.; Yamamoto, K. *Angew. Chem., Int. Ed.* **2015**, *54*, 1.
- (7) (a) Forrest, S. R.; Thompson, M. E. *Chem. Rev.* **2007**, *107*, 923. (b) Kato, S.; Shimizu, S.; Taguchi, H.; Kobayashi, A.; Tobita, S.; Nakamura, Y. *J. Org. Chem.* **2012**, *77*, 9120. (c) Yang, S.; Guan, D.; Yang, M.; Tian, J.; Chu, W.; Sun, Z. *Tetrahedron Lett.* **2015**, *56*, 2223.
- (8) Kato, S.; Shimizu, S.; Taguchi, H.; Kobayashi, A.; Tobita, S.; Nakamura, Y. *J. Org. Chem.* **2012**, *77*, 9120.
- (9) (a) Wang, H. Y.; Liu, F.; Xie, L. H.; Tang, C.; Peng, B.; Huang, W.; Wei, W. *J. Phys. Chem. C* **2011**, *115*, 6961. (b) Niu, F.; Niu, H.; Liu, Y.; Lian, J.; Zeng, P. *RSC Adv.* **2011**, *1*, 415.
- (10) (a) Tomkeviciene, A.; Grazulevicius, J. V.; Kazlauskas, K.; Gruodis, A.; Jursenas, S.; Ke, T. H.; Wu, C. C. *J. Phys. Chem. C* **2011**, *115*, 4887. (b) Gong, S.; Zhao, Y.; Yang, C.; Zhong, C.; Qin, J.; Ma, D. *J. Phys. Chem. C* **2010**, *114*, 5193. (c) Kanibolotsky, A. L.; Perepichkaz, I. F.; Skabara, P. J. *Chem. Soc. Rev.* **2010**, *39*, 2695.
- (11) Gong, W. L.; Zhong, F.; Aldred, M. P.; Fu, Q.; Chen, T.; Huang, D. K.; Shen, Y.; Qiao, X. F.; Ma, D.; Zhu, M. Q. *RSC Adv.* **2012**, *2*, 10821.
- (12) Kochaprastit, P.; Prachumrak, N.; Tarsang, R.; Keawin, T.; Jungsuttiwong, S.; Sudyoadsuk, T.; Promarak, V. *Tetrahedron Lett.* **2013**, *54*, 3683.
- (13) Gong, W. L.; Wang, B.; Aldred, M. P.; Li, C.; Zhang, G. F.; Chem, T.; Wang, L.; Zhu, M. Q. *J. Mater. Chem. C* **2014**, *2*, 7001.
- (14) (a) Liu, F.; Tang, C.; Chen, Q. Q.; Li, S. Z.; Wu, H. B.; Xie, L. H.; Peng, B.; Wei, W.; Cao, Y.; Huang, W. *Org. Electron.* **2009**, *10*, 256. (b) Kumchoo, T.; Promarak, V.; Sudyoadsuk, T.; Sukwattanasinitt, M.; Rashatasakhon, P. *Chem.—Asian J.* **2010**, *5*, 2162. (c) Tao, S.; Zhou, Y.; Lee, C. S.; Zhang, X.; Lee, S. T. *Chem. Mater.* **2010**, *22*, 2138. (d) Ali, F.; Periasamy, N.; Patankar, M. P.; Narasimhan, K. L. *J. Phys. Chem. C* **2011**, *115*, 2462. (e) Thomas, K. R. J.; Kapoor, N.; Bolisetty, M. N. K. P.; Jou, J. H.; Chen, Y. L.; Jou, Y. C. *J. Org. Chem.* **2012**, *77*, 3921. (f) Chen, S.; Wei, J.; Wang, K.; Wang, C.; Chen, D.; Liu, Y.; Wang, Y. *J. Mater. Chem. C* **2013**, *1*, 6594. (g) Usluer, O. *J. Mater. Chem. C* **2014**, *2*, 8098.
- (15) (a) Grazulevicius, J. V.; Strohriegel, P.; Pielichowski, J.; Pilichowski, K. *Prog. Polym. Sci.* **2003**, *28*, 1297. (b) Morin, J. F.; Leclerc, M.; Adès, D.; Siove, A. *Macromol. Rapid Commun.* **2005**, *26*, 761.
- (16) (a) Tsai, M. H.; Ke, T. H.; Lin, H. W.; Wu, C. C.; Chiu, S. F.; Fang, F. C.; Liao, Y. L.; Wong, K. T.; Chen, Y. H.; Wu, C. I. *ACS Appl. Mater. Interfaces* **2009**, *1*, 567. (b) Tao, Y.; Wang, Q.; Yang, C.; Zhang, C.; Zhang, K.; Qin, J.; Ma, D. *Adv. Funct. Mater.* **2010**, *20*, 304. (c) Mizuno, Y.; Takasu, I.; Uchikoga, S.; Enomoto, S.; Sawabe, T.; Amano, A.; Wada, A.; Sugizaki, T.; Yashida, J.; Ono, T.; Adachi, C. *J. Phys. Chem. C* **2012**, *116*, 20681. (d) Cui, L. S.; Liu, Y.; Yuan, X. D.; Li, Q.; Jiang, Z. Q.; Liao, L. S. *J. Mater. Chem. C* **2013**, *1*, 8177. (e) Du, X.; Huang, Y.; Tao, S.; Yang, X.; Wu, C.; Wei, H.; Chan, M. Y.; Yan, V. W. *Chem.—Asian J.* **2014**, *9*, 1500. (f) Shi, H.; Xin, D.; Dong, X.; Dai, J. X.; Wu, X.; Miao, Y.; Fang, L.; Wang, H.; Choi, M. M. F. *J. Mater. Chem. C* **2014**, *2*, 2160. (g) Cheng, S. H.; Hung, W. Y.; Cheng, M. T.; Chen, H. F.; Chaskar, A.; Lee, G. H.; Chou, S. H.; Wong, K. T. *J. Mater. Chem. C* **2014**, *2*, 8554. (h) Yuan, X. D.; Liang, J.; He, Y. C.; Li, Q.; Zhang, C.; Jiang, Z. Q.; Liao, L. S. *J. Mater. Chem. C* **2014**, *2*, 8736. (i) Tang, C.; Bi, R.; Tao, Y.; Wang, F.; Cao, X.; Wang, S.; Jiang, T.; Zhang, C.; Zhang, H.; Huang, W. *Chem. Commun.* **2015**, *51*, 1650. (j) Rothmann, M. M.; Haneder, S.; Como, E. D.; Lennartz, C.; Schidknecht, C.; Strohriegel, P. *Chem. Mater.* **2010**, *22*, 2403. (k) Wagner, D.; Hoffmann, S. T.; Heinemeyer, U.; Münster, I.; Köhler, A.; Strohriegel, P. *Chem. Mater.* **2013**, *25*, 3758. (l) Bagnich, S. A.; Athanasopoulos, S.; Rudnick, A.; Schroegele, P.; Bauer, I.; Greenham, N. C.; Strohriegel, P.; Köhler, A. *J. Phys. Chem. C* **2015**, *119*, 2380. (m) Sonntag, M.; Strohriegel, P. *Chem. Mater.* **2004**, *16*, 4736.
- (17) Huang, H.; Fu, Q.; Pan, B.; Zhuang, S.; Wang, L.; Chen, J.; Ma, D.; Yang, C. *Org. Lett.* **2012**, *14*, 4786.
- (18) (a) Boudreault, P. L. T.; Wakim, S.; Tang, M. L.; Tao, Y.; Bao, Z.; Leclerc, M. *J. Mater. Chem.* **2009**, *19*, 2921. (b) Cheedarala, R. K.; Kim, G. H.; Cho, S.; Lee, J.; Kim, J.; Song, H. K.; Kim, I. Y.; Yang, C. *J. Mater. Chem.* **2011**, *21*, 843. (c) Mutkins, K.; Chen, S. S. Y.; Pivrikas, A.; Aljada, M.; Burn, P. L.; Meredith, P.; Powell, B. J. *Polym. Chem.* **2013**, *4*, 916. (d) Montoya, M. M.; Oritz, R. P.; Curiel, D.; Spinosa, A. E.; Allain, A.; Facchetti, A.; Marks, T. J. *J. Mater. Chem. C* **2013**, *1*, 1959. (e) Tomkeviciene, A.; Grazulevicius, J. V.; Volyniuk, D.; Jankauskas, V.; Sini, G. *Phys. Chem. Chem. Phys.* **2014**, *16*, 13932. (f) Sonntag, M.; Kreger, K.; Hanft, D.; Strohriegel, P. *Chem. Mater.* **2005**, *17*, 3031.
- (19) (a) Ooyama, Y.; Nagano, T.; Inoue, S.; Imae, I.; Komaguchi, K.; Ohshita, J.; Harima, Y. *Chem.—Eur. J.* **2011**, *17*, 14837. (b) Lee, W.; Cho, N.; Won, J. K.; Ko, J.; Hong, J. I. *Chem.—Asian J.* **2012**, *7*, 343. (c) Chu, H. C.; Sahu, D.; Hsu, C. Y.; Podhy, H.; Patra, D.; Lin, J. T.; Bhattacharya, D.; Lu, K. L.; Wei, K. H.; Lin, H. C. *Dyes Pigm.* **2012**, *94*, 1488. (d) Thongkasee, P.; Thangthong, A.; Janthasing, N.; Sudyoadsuk, T.; Naumuangruk, S.; Keawin, T.; Jungsuttiwong, S.; Promarak, V. *ACS Appl. Mater. Interfaces* **2014**, *6*, 8212. (e) Su, J. Y.; Lo, C. Y.; Tsai, C. H.; Chen, C. H.; Chou, S. H.; Liu, S. H.; Chou, P. T.; Wong, K. T. *Org. Lett.* **2014**, *16*, 3176. (f) Pearson, A. J.; Watters, D. C.; Yi, H.; Sorjadi, M. S.; Reynolds, L. X.; Marchisio, P. P.; Kingsley, J.; Haque, S. A.; Iraqi, A.; Lidzey, D. G. *RSC Adv.* **2014**, *4*, 43142.

- (20) (a) Venkateswarao, A.; Thomas, K. R. J.; Lee, C. P.; Ho, K. C. *Tetrahedron Lett.* **2013**, *54*, 3985. (b) Venkateswarao, A.; Thomas, K. R. J.; Lee, C. P.; Lee, C. T.; Ho, K. C. *ACS Appl. Mater. Interfaces* **2014**, *6*, 2528.
- (21) (a) Zhang, Y.; Wang, L.; Wada, T.; Sasabe, H. *Macromolecules* **1996**, *29*, 1569. (b) Zhang, Y.; Wang, L.; Wada, T.; Sasabe, H. *Chem. Mater.* **1997**, *9*, 2798. (c) Hwang, J.; Sohn, J.; Park, S. Y. *Macromolecules* **2013**, *36*, 7970. (d) Hofmann, U.; Grasruck, M.; Leopold, A.; Schreiber, A.; Schlöter, S.; Hohle, C.; Strohrriegel, P.; Haarer, D.; Zilker, S. *J. Phys. Chem. B* **2010**, *104*, 3887.
- (22) (a) Chang, C. C.; Wu, J. Y.; Chien, C. W.; Wu, S.; Liu, H.; Kang, C. C.; Yu, Chang, T. C. *Anal. Chem.* **2003**, *75*, 6177. (b) Gee, H. C.; Lee, C. H.; Jeang, Y. H.; Jang, W. D. *Chem. Commun.* **2011**, *47*, 11963. (c) Goswami, S.; Paul, S.; Manna, A. J. *Chem. Soc., Dalton Trans.* **2013**, *42*, 10682. (d) Feng, X. J.; Tian, P. Z.; Xu, Z.; Chen, S. F.; Wang, M. S. *J. Org. Chem.* **2013**, *78*, 11318. (e) Konidena, R. K.; Thomas, K. R. J. *RSC Adv.* **2014**, *4*, 22902.
- (23) Jiang, H.; Sun, J. *New J. Chem.* **2013**, *37*, 3161.
- (24) (a) Kong, K.; Xiao, L.; Liu, Y.; Chen, Z.; Qu, B.; Gong, Q. *New J. Chem.* **2010**, *34*, 1994. (b) Park, Y.; Kim, B.; Lee, C.; Hyun, A.; Jang, S.; Lee, J. H.; Gal, Y. S.; Kim, J. Y.; Kim, K. S.; Park, J. *J. Phys. Chem. C* **2011**, *115*, 4843. (c) Hua, Y.; Chang, S.; Huang, H.; Zhou, X.; Zhu, X.; Zhao, J.; Chen, T.; Wong, W. Y.; Wong, W. K. *Chem. Mater.* **2013**, *25*, 2146. (d) Yao, L.; Sun, S.; Xue, S.; Zhang, S.; Wu, X.; Zhang, H.; Pan, Y.; Gu, C.; Li, F.; Ma, Y. *J. Phys. Chem. C* **2013**, *117*, 14189–14196. (e) Janaka, H.; Shizu, K.; Nakanotani, H.; Adachi, C. *J. Phys. Chem. C* **2014**, *118*, 15985. (f) Tian, Q.; Yang, X.; Cheng, M.; Wong, H.; Sun, L. *J. Phys. Chem. C* **2014**, *118*, 16851. (g) Huang, Z. S.; Feng, H. L.; Zong, X. F.; Iqbal, Z.; Zeng, H.; Kuang, D. B.; Wang, L.; Meier, H.; Cao, D. *J. Mater. Chem. C* **2014**, *2*, 15365. (h) Bodedla, G. B.; Thomas, K. R. J.; Li, C. T.; Ho, K. C. *RSC Adv.* **2014**, *4*, 53588. (i) Ananthakrishnan, J. S.; Varathan, E.; Subramanian, V.; Somanathan, N.; Mandal, A. B. *J. Phys. Chem. C* **2014**, *118*, 28084–28094. (j) Lai, R. Y.; Kong, X.; Janekhe, S. A.; Bard, A. J. *J. Am. Chem. Soc.* **2003**, *125*, 12631. (k) Kulkarni, A. P.; Wu, P. T.; Kwon, T. W.; Jenekhe, S. A. *J. Phys. Chem. B* **2005**, *109*, 19584. (l) Kong, X.; Kulkarni, A. P.; Jenekhe, S. A. *Macromolecules* **2003**, *36*, 8992. (m) Kulkarni, A. P.; Kong, X.; Jenekhe, S. A. *Macromolecules* **2006**, *39*, 8699. (n) Lai, R. Y.; Fabrizio, E. F.; Lu, L.; Jenekhe, S. A.; Bard, A. J. *J. Am. Chem. Soc.* **2001**, *123*, 9112. (o) Jenekhe, S. A.; Lu, L.; Alam, M. M. *Macromolecules* **2001**, *34*, 7315. (p) Reghu, R. R.; Grazulevicius, V. J.; Simokaitiene, J.; Data, P.; Karon, K.; Lapkowski, M.; Gaidelis, V.; Jankauskas, V. *J. Phys. Chem. C* **2012**, *116*, 15878.
- (25) Sun, J.; Jiang, H. J.; Zhang, J. L.; Tao, Y.; Chen, R. F. *New J. Chem.* **2013**, *37*, 977.
- (26) Hauck, M.; Turdean, R.; Memminger, K.; Schönhaber, J.; Rominger, F.; Müller, T. J. *J. Org. Chem.* **2010**, *75*, 8591.
- (27) (a) Franz, A. W.; Rominger, F.; Müller, T. J. *J. Org. Chem.* **2008**, *73*, 1795. (b) Li, Y.; Feng, J. K.; Ren, A. M. *J. Org. Chem.* **2005**, *70*, 5987. (c) Franz, A. W.; Popa, L. N.; Rominger, F.; Müller, T. J. *J. Org. Biomol. Chem.* **2009**, *7*, 469.
- (28) (a) Barkschat, C. S.; Stoychera, S.; Himmelhaus, M.; Müller, T. J. *J. Chem. Mater.* **2010**, *22*, 52. (b) Sailer, M.; Nonnenmacher, M.; Oesar, T.; Müller, T. J. *Eur. J. Org. Chem.* **2006**, 423. (c) Sailer, M.; Gropeanu, R. A.; Müller, T. J. *J. Org. Chem.* **2003**, *68*, 7509. (d) Hauck, M.; Schönhaber, J.; Zuccherro, A. J.; Hardcastle, K. I.; Müller, T. J.; Bunz, U. H. F. *J. Org. Chem.* **2007**, *72*, 6714. (e) Mayer, T.; Ogermann, D.; Pankrath, A.; Kleinermanns, K.; Müller, T. J. *J. Org. Chem.* **2012**, *77*, 3704. (f) Krämer, C. S.; Zeitler, K.; Müller, T. J. *J. Org. Lett.* **2000**, *2*, 3723. (g) Krain, M.; Oesar, T.; Müller, T. J. *J. Org. Lett.* **2008**, *10*, 2797. (h) Krämer, C. S.; Müller, T. J. *Eur. J. Org. Chem.* **2003**, 3534. (i) Krämer, C. S.; Zeitler, K.; Müller, T. J. *Tetrahedron Lett.* **2001**, *42*, 8619.
- (29) (a) Stille, J. K. *Angew. Chem., Int. Ed. Engl.* **1986**, *98*, 504. (b) Daub, J.; Engl, R.; Kurzawa, S.; Miller, S. E.; Schneider, S.; Stockmann, A.; Wasielewski, M. R. *J. Phys. Chem. A* **2001**, *105*, S655.
- (30) (a) Morin, J. F.; Leclerc, M. *Macromolecules* **2001**, *34*, 4680. (b) Morin, J. F.; Leclerc, M. *Macromolecules* **2002**, *35*, 8413. (c) Fu, Y.; Bo, Z. *Macromol. Rapid Commun.* **2005**, *26*, 1704.
- (31) Reichardt, C. *Chem. Rev.* **1994**, *94*, 2319.
- (32) Tyagi, P.; Venkateswarao, A.; Thomas, K. R. J. *J. Org. Chem.* **2011**, *76*, 4571.
- (33) Panthi, K.; Adhikari, R. M.; Kinstle, T. H. *J. Phys. Chem. A* **2010**, *114*, 4550.
- (34) Sung, J.; Kim, P.; Lee, Y. O.; Kim, J. S.; Kim, D. *J. Phys. Chem. Lett.* **2011**, *2*, 818.
- (35) Subuddhi, U.; Halder, S.; Sankararaman, S.; Mishra, A. K. *Photochem. Photobiol. Sci.* **2006**, *5*, 459.
- (36) (a) Mes, G. F.; Jong, B. D.; Ramesdonk, H. J. V.; Verhoeven, J. W.; Warman, J. M.; Haas, M. P. D.; Dool, L. E. W. H. *J. Am. Chem. Soc.* **1984**, *106*, 6524. (b) Manohara, S. R.; Udaya Kumar, V.; Shivakumaraiah; Gerward, L. *J. Mol. Liq.* **2013**, *181*, 97.
- (37) Frisch, M. J.; Trucks, G. H.; Schlegel, H. B.; Scuseria, G. E.; Robb, M. A.; Cheeseman, J. R.; Scalmani, G.; Barone, V.; Mennucci, B.; Petersson, G. A.; Nakatsuji, H.; Caricato, M.; Li, X.; Hratchian, H. P.; Izmaylov, A. F.; Bloino, J.; Zheng, G.; Sannenger, J. L.; Hada, M.; Ehara, M.; Toyota, K.; Fukuda, R.; Hasegawa, J.; Ishida, M.; Nakajima, T.; Honda, Y.; Kitao, O.; Nakai, H.; Vreven, T.; Montgomery, J. A.; Peralta, J. E., Jr.; Ogliaro, F.; Bearpark, M.; Heyd, J. J.; Brothers, E.; Kudin, K. N.; Staroverov, V. N.; Kobayashi, R.; Normand, J.; Raghavachari, K.; Rendell, A.; Burant, J. C.; Iyengar, S. S.; Tomasi, J.; Cossi, M.; Rega, N.; Millam, J. M.; Klene, M.; Knox, J. E.; Cross, J. B.; Bakken, V.; Adamo, C.; Jaramillo, J.; Gomperts, R.; Stratmann, R. E.; Yazyev, O.; Austin, A. J.; Cammi, R.; Pomelli, C.; Ochterski, J. W.; Martin, R. L.; Morokuma, K.; Zakrzewski, V. G.; Voth, G. A.; Salvador, P.; Dannenberg, J. J.; Dapprich, S.; Daniels, A. D.; Farkas, O.; Foresman, J. B.; Ortiz, J. V.; Cioslowski, J.; Fox, D. J. *Gaussian 09*, revision A.02; Gaussian, Inc.: Wallingford, CT, 2009.
- (38) (a) Becke, A. D. *J. Chem. Phys.* **1993**, *98*, 1372. (b) Lee, C.; Yang, W.; Parr, G. *Phys. Rev. B* **1988**, *37*, 785.
- (39) (a) Marcus, R. A. *J. Chem. Phys.* **1956**, *24*, 966. (b) Hush, N. S. *J. Chem. Phys.* **1958**, *28*, 962. (c) Marcus, R. A. *Rev. Mod. Phys.* **1993**, *65*, 599.
- (40) (a) Nelsen, S. F.; Wolff, J. J.; Chang, H.; Powell, D. P. *J. Am. Chem. Soc.* **1991**, *113*, 7882. (b) Nelsen, S. F.; Blomgren, F. *J. Org. Chem.* **2001**, *66*, 6551.
- (41) (a) Ran, X. Q.; Feng, J. K.; Ren, A. M.; Li, W. C.; Zou, L. Y.; Sun, C. C. *J. Phys. Chem. A* **2009**, *113*, 7933. (b) Yin, J.; Chen, R. F.; Zhang, S. L.; Ling, Q. D.; Huang, W. J. *J. Phys. Chem. A* **2010**, *114*, 3655. (c) Cias, P.; Slugovc, S.; Gescheidt, G. *J. Phys. Chem. A* **2011**, *115*, 14519. (d) Yao, Y.; Tao, M. K.; Chen, R. F.; Zheng, C.; An, Z. F.; Huang, W. *RSC Adv.* **2012**, *2*, 7860. (e) Varathan, E.; Vijay, D.; Kumar, P. S. V.; Subramanian, V. *J. Mater. Chem. C* **2013**, *1*, 4261. (f) Varathan, V.; Vijay, D.; Subramanian, V. *J. Phys. Chem. C* **2014**, *118*, 21741.
- (42) (a) Vetrichelvan, M.; Nagarajan, R.; Veliyaveetil, S. *Macromolecules* **2006**, *39*, 8303. (b) Zheng, Q.; Chen, S.; Zhang, B.; Wang, L.; Tang, C.; Katz, H. E. *Org. Lett.* **2011**, *13*, 324.